J|A|C|S
ARTICLES
Published on Web 01/31/2007

Synchronous Photoinitiation of Endothelial NO Synthase Activity by a Nanotrigger Targeted at Its NADPH Site

Edward Beaumont,[†,‡] Jean-Christophe Lambry,[†,‡] Clément Gautier,[†,‡] Anne-Claire Robin,[§] Said Gmouh,[§] Vladimir Berka,[||] Ah-Lim Tsai,[||] Mireille Blanchard-Desce,[§] and Anny Slama-Schwok*[,†,‡]

Contribution from the Unité 696, INSERM, Palaiseau France, Laboratory for Optics and Biosciences, UMR CNRS 7645, Ecole Polytechnique, Palaiseau, France, Photonique Moléculaire, UMR CNRS 6510, Université de Rennes I, France, and Division of Hematology, Internal Medicine, University of Texas Houston Medical School, Houston, Texas

Received October 25, 2006; E-mail: Anny.Schwok@polytechnique.edu

Abstract: We designed a new nanotrigger to synchronize and monitor an enzymatic activity interacting specifically with the conserved NADPH binding site. The nanotrigger (NT) combines a docking moiety targeting the NADPH site and a chromophore moiety responsive to light excitation for efficient electron transfer to the protein. Specific binding of the nanotrigger to the reductase domain of the endothelial nitric oxide synthase (eNOSred) was demonstrated by competition between NADPH and the nanotrigger on the reduction of eNOSred flavin. A micromolar K_i was estimated. We had monitored initiation of eNOSred activity by ultrafast transient spectroscopy. The transient absorption spectrum recorded at 250 ps fits the expected sum of the reduced and oxidized species, independently obtained by other chemical methods, in agreement with a photoinduced electron transfer from the excited nanotrigger to the flavin moiety of eNOSred. The rate of electron transfer from the excited state of the nanotrigger (NT*) to the protein is estimated to be $k_{ET} = (7 \pm 2) \times 10^9\ s^{-1}$ using the decay of oxidized eNOSred-bound nanotrigger compared against prereduced eNOSred or glucose 6-P dehydrogenase as controls. This fast electron transfer bypasses the slow hydride transfer to initiate NOS catalysis as shown by ultrafast kinetics using the eNOSred mutated in the regulatory F1160 residue. The selective targeting of the nanotrigger to NADPH sites should allow controlled initiation of the enzymatic activity of numerous proteins containing an NADPH site.

Introduction

A better understanding of protein functions and interactions often requires the ability to trigger and initiate a specific biological activity. In the past years, "caged nucleotides" have been developed to trigger an enzymatic activity with light. These compounds are derivatives of a natural protein cofactor, such as ATP or NADPH, in which light activation leads to cleavage of the "caging" moiety.[1−2] The released cofactor is then free to diffuse toward its binding site within the protein. Actually, the intrinsic limitation of these compounds to millisecond timescales originates from the rate of diffusion of the active moiety to the catalytic site in the protein, especially with proteins with high catalytic turnover.[3] Recently, such caged compounds have been used with multiphotonic excitation[4] and coupled to an inhibitor of the inducible NO synthase (iNOS).[5] The molecular wires developed in the group of H. Gray were designed to drive enzymatic reactions with light, and the approach was applied to the cytochrome P450 and more recently to iNOS.[6−7] The Re or Ru organometallic complex is tethered to a heme binding moiety such as imidazole or an enzyme substrate.[6−7] Although the electron transfer occurred within 300 ps upon 355 nm excitation, it was not related to a physiological activation of iNOS, and in some cases, the wire inactivated the protein by sterically hindering its active dimer formation.

Thus, the innovative device that triggers and synchronizes biological molecules in their native state "instantaneously" both in time and in space would set the "zero" time of the catalysis and thus allow time-resolved measurements of the enzymatic activity in an ensemble of molecules. In this work, we develop a novel approach to trigger enzymatic activity by light in a synchronous manner. We designed a nanotrigger possessing two main characteristics. The first one is the specific targeting of the nanotrigger to the NADPH site within proteins. The second

[†] Unité 696, INSERM.
[‡] Ecole Polytechnique.
[§] Université de Rennes I.
[||] University of Texas Houston Medical School.

(1) Stoddard, B. L.; Cohen, B. E.; Brubaker, M.; Mesecar, A. D.; Koshland, D. E. *Nat. Struct. Biol.* **1998**, *5*, 891−897.
(2) Salerno, C. P.; Magde, D.; Patron, A. P. *J. Org. Chem.* **2000**, *65*, 3971−3981.
(3) Ursby, T.; Weik, M.; Fioravanti, E.; Delarue, M.; Goeldner, M.; Bourgeois, D. *Acta Crystallogr., Sect. D* **2002**, *58*, 607−14.
(4) Allin, C.; Ahmadian, M. R.; Wittinhofer, A.; Gewert, K. *Proc Natl. Acad. Sci. U.S.A.* **2001**, *98*, 7754−9.
(5) Perdicakis, B.; Montgomery, H. J.; Abbott, G. L.; Fishlock, D.; Lajoie, G. A.; Guillemette, J. G.; Jervis, E. *Bioorg. Med. Chem.* **2005**, *13* (1), 47−57.
(6) Dunn, A.; Dmochowski, I. J.; Winkler, J. R.; Gray, H. B. *J. Am. Chem. Soc.* **2003**, *125*, 12450−12456.
(7) Bellinston-Bittner, W.; Dunn, A. R.; Le Nguyen, Y. H.; Stuehr, D. J.; Winkler, J. R.; Gray, H. B. *J. Am. Chem. Soc.* **2005**, *127*, 15907−15915.

10.1021/ja067543e CCC: $37.00

Scheme 1. Design of the Nanotrigger

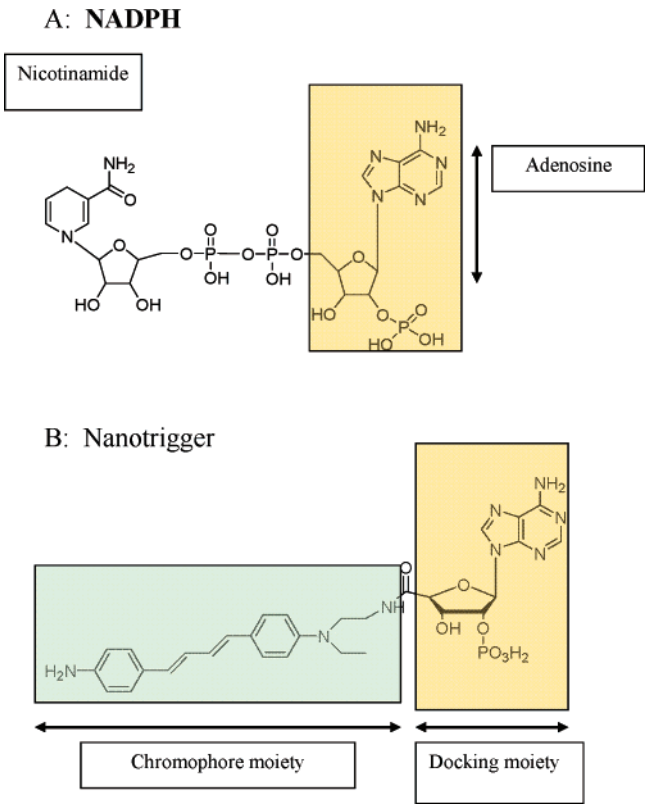

characteristic is the ability to trigger the redox reaction leading to the enzymatic activity by a short laser pulse. This nanotrigger is a photoactivatable analogue of NADPH and should interact specifically with the NADPH site, present in numerous proteins, without the limitation of diffusion as encountered by the caged NADPH. Moreover, the catalysis would be rapidly initiated at the native state of the enzyme, and time-resolved spectroscopy can be applied to record the kinetic steps.

The design of the nanotrigger was based on the conserved motifs of the ubiquitous NADPH binding sites. Crystallographic data of NADPH-containing proteins[8−9] showed that the main recognition motifs of NADPH in its binding site are found in the nucleotidic part, with the sugar, adenine rings, and the final phosphate linked by numerous H-bonding interactions with the proteins, in particular by means of a highly conserved arginine residue.[8−10] The nicotinamide subunit of NADPH is on the other hand often flexible, closer to the solvent interface, and its recognition within the NADPH site is quite variable among various proteins (Scheme 1A). NADPH can adopt an extended conformation with the adenine and nicotinamide rings assuming a perpendicular orientation and an end-to-end distance of roughly 15 Å. Alternatively, NADPH can assume a fold back conformation by the nicotinamide moiety stacking on the purine ring.[11−12] In other instances, coupled motions of the nicotinamide and an aromatic residue have been suggested.[13] These motions are often involved in the regulation of the catalysis, as for example at the level of nNOS, Phe1395 by blocking access to FAD.[12] Thus, any designed molecule should overcome this physical blockage and rapidly direct the photoinduced electron transfer to the natural electron acceptor, FAD, in the case of nNOS.

Our design conserved the nucleotide recognition motif of NADPH. This should confer the proper binding of the nanotrigger to the NADPH site. The nicotinamide part was replaced by a chromophore moiety, which, upon photoactivation, should transfer electron(s) to the flavin center of the protein and initiate the catalysis by selective light excitation (Scheme 1B). Preliminary modeling studies optimized both the nature and the length of the conjugated chromophore to fit in the NADPH cavity of the cytochrome P450 reductase.[13−14] Moreover, an extended conformation of the nanotrigger by means of conjugated double bonds and a peptidic linker between chromophore and nucleotidic moieties could "lock" the enzyme in an active conformation, favorable for the electron transfer. The extended conformation of the nanotrigger should also maximize the delocalization of the π electrons on the chromophore, with subsequent favorable properties of one and two photon absorption.[14−16] In this work, the proof of concept was tested on the reductase domain of the endothelial nitric oxide synthase, eNOSred, [17] highly homologous to nNOSred and P450 reductase. First, the specific binding of the nanotrigger to the NADPH site was demonstrated by measuring the rate of flavin reduction by NADPH in stopped-flow experiments. These data showed a competitive binding of the nanotrigger and NADPH in the cofactor binding site. Moreover, the photophysical and photochemical characteristics of the bound nanotrigger to eNOSred were measured by ultrafast transient absorption in pump−probe experiments. The transient spectrum recorded 250 ps after the pulse fits the expected sum of the reduced and oxidized species, independently obtained by another chemical method (reduction with $SbCl_5$). The decay of the transient absorption of the nanotrigger bound to eNOSred was enhanced relative to the control, and the rate of the electron transfer was estimated to be $k_{ET} = (7 \pm 2) \times 10^9\ s^{-1}$. Moreover, steady-state irradiation also showed that nanotrigger NT triggering allowed subsequent heme reduction of WT nNOS that became (partly) nitrosylated in the presence of Ca^{2+}/calmodulin. Thus, our novel nanotrigger initiated eNOS activity in a synchronous manner by light.

Materials and Methods

Materials: NADPH (99.8% purity), Tris-HCl, potassium ferricyanide, glycerol, and EDTA were purchased from Sigma. High purity argon (99.9995%) was obtained from Alpha Gas.

Synthesis: The nanotrigger (NT) was prepared as described in Scheme 2.[15] A coupling reaction between the chromophoric moiety **A** and the adenosine moiety **B** was first performed. The acetal protection was then removed with trifluoroacetic acid, and a phosphate group was

(8) Carugo, O.; Argos, P. *Proteins* **1997**, *28*, 10−28.
(9) Duax, W. D.; Pletnev, V.; Addlagatta, A.; Bruenn, J.; Weeks, C. M. *Proteins: Struct., Funct., Genet.* **2003**, *53*, 931−943.
(10) Tiso, M.; Konas, D. W.; Panda, K.; Garcin, E. D.; Sharma, M.; Getzoff, E. D.; Stuehr, D. J. *J. Biol. Chem.* **2005**, *280*, 39208−39219.
(11) Malito, E.; Alfieri, A.; Frasije, M. W.; Mattevi, A. *Proc Natl. Acad. Sci. U.S.A.* **2004**, *101*, 13157−62.
(12) Garcin, E. D.; Bruns, C. M.; Lloyd, S. J.; Hosfield, D. J.; Tiso, M.; Gachhui, R.; Stuehr, D. J.; Tainer, J. A.; and Getzoff, E. D. *J. Biol. Chem.* **2004**, *279*, 37918−37927.
(13) Zhang, J.; Martasek, P.; Paschke, R.; Shea, T.; Silver Masters, B. S.; Kim, J. J. *J. Biol. Chem.* **2001**, *276*, 37506−13.
(14) The molecular modeling of NT in P450 reductase will be detailed elsewhere (Slama-Schwok, A. and Lebret, M.).
(15) The detailed synthesis is described elsewhere (Robin, A. C.; Gmouh. S.; Mongin, O.; Jouikov, V.; Werts, M. H. V.; Gautier, C.; Slama-Schwok, A.; Blanchard-Desce, M. Submitted). A french patent was deposited No. 0511914: Synchronous trigger of the catalysis of NADPH enzymes by a photoactivable analog of NADPH: A. Slama-Schwok, M. Blanchard-Desce, S. Gmouh, J.-L. Martin.

Scheme 2. Synthetic Route to Nanotrigger NT[a]

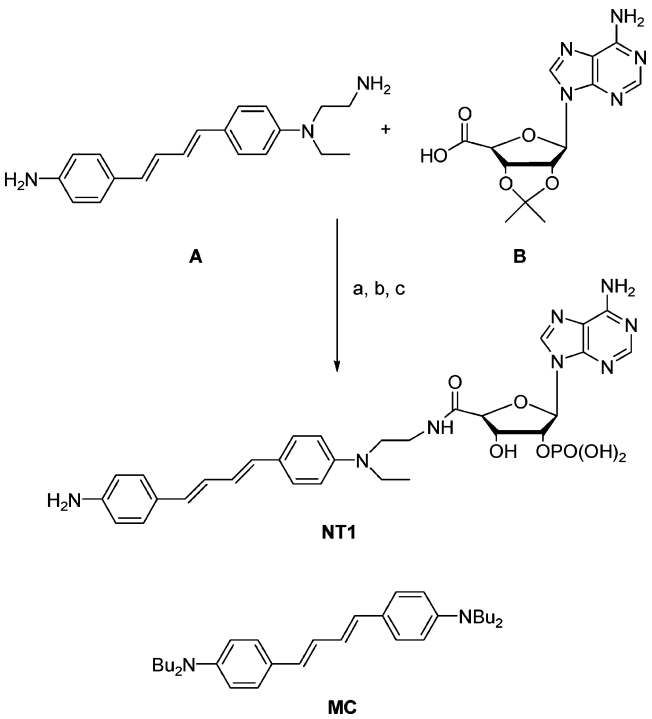

[a] Reagents and conditions: (a) HBTU/DMF/Et_3N; (b) TFA/THF/H_2O; (c)(i) $i(Pr)_2N-P(OBn)_2$/tetrazole, (ii) O_2/CH_2Cl_2, (iii) Me_3SiBr/CH_2Cl_2.

inserted with dibenzyldiisopropylphosphoramidite. The resulting phosphoramidate was oxidized, and the benzyl protective groups were removed using bromotrimethylsilane to afford NT as a mixture of two isomers (phosphate group on the 2 or 3 hydroxyl of the sugar). A lipophilic model chromophore (MC) has been used for electrochemical characterization in solution performed in a similar way as described.[16]

Expression of the Enzymes. The eNOS reductase domain was overexpressed in yeast and purified as reported previously.[17] F1160A mutant was prepared by site-directed mutagenesis in the lab of Dr. Tsai, UTH MS. Purified nNOS was purchased from Calbiochem. Purified glucose 6-phosphate dehydrogenase (Baker yeast) was purchased from Sigma.

Preparation of Samples for Stopped-Flow Measurements: Argon-saturated solutions of 20 μM eNOSred alone or in the presence of the nanotrigger were prepared apart from oxygen-free solutions of NADPH (200 μM to 10 mM) and used for stopped-flow experiments. Removing oxygen provided a better stability of the reducing agent. The stopped-flow experiments were performed on an Edinburgh apparatus with single wavelength detection at 455 nm or 340 nm with a dead time of about 2 ms. The absorption decays were usually monitored at 1, 5, and 10 s time scales. The data have been fitted by three exponentials and a constant term using the Origin software.

Preparation of Samples for Ultrafast Kinetics. A concentrated solution of proteins (10 to 20 μM) in 50 mM Tris-HCl buffer containing 150 mM NaCl at pH = 7.5 and 5% glycerol was mixed with the NT in an optical cuvette with a 1 mm path length. The extent of prereduction achieved by light irradiation of an air-free solution of eNOSred containing 5 mM EDTA was assessed by calculating the ratio of the OD at 455 nm.[18] We succeeded to obtain fully reduced eNOSred indicated by a maximal decrease of A_{455}. However, the subsequent addition of NT to the reduced protein caused unavoidable partial reoxidation of the flavin thus yielded maximally a 60% net reduction.

Time-Resolved Spectroscopy. Multicolor pump−probe spectroscopy was performed with a 500-Hz setup based on a home-built TiSa oscillator and a 1-kHz regenerative amplifier (Spitfire, Spectra Physics), delivering 50-fs 0.5 mJ at 810 nm. A synchronized chopper allowed a reduction of the repetition rate to 500 Hz. Pump pulses centered at 405 nm were generated with a 0.5 mm BBO crystal used in the SHG configuration. White light probe pulses ranging from 430 to 700 nm were generated by focusing part of the fundamental on a CaF_2 window and separated in test and reference beams. These beams were, after passing through the sample, dispersed and detected shot-by-shot on a CCD camera configured as a dual-array detector. The sample was renewed between subsequent pulse pairs by rotation perpendicularly to the beams. 10 scans were usually recorded in a single experiment in two timescales: 1−10 ps and 10−600 ps. An average of three experiments was used for Figure 5. Carbon monoxide bound to reduced myoglobin was a reference for an undecaying signal at 200−600 ps.[19] Analysis of the data was performed by singular value decomposition (SVD) of the time−wavelength matrix and by exponential fit of the single wavelength data.

Results

1. Competition between the Nanotrigger and NADPH for the NADPH Site of eNOSred. The reductase domain of eNOS contains 1 equiv of FAD and FMN and binds NADPH very similarly to the case of cytochrome P450 reductase (CPR). Detailed stopped-flow studies on CPR have been reported.[20−21] Previous studies on nNOS[22−26] showed that FAD reduction by NADPH occurs in three distinct kinetic steps. In the first step, NADPH binds to the enzyme; the second step involves a hydride transfer from NADPH to FAD, with the third one being an intramolecular electron transfer between the two flavins. The rebinding of the oxidized $NADP^+$ is inhibitory to steps two and/or three, whose rates depend upon $NADP^+$ release. We hypothesized that closely related eNOS would undergo qualitatively similar binding and reduction steps as those for nNOS. Thus, our nanotrigger should interfere with NADPH binding in the first step and affect the second and third kinetic steps as well. We used the isolated reductase domain of eNOS in this study.[17] The flavin reduction was monitored at 455 nm after rapid mixing with either NADPH alone or NADPH in the presence of nanotrigger. Absorption changes at 340 nm due to NADPH consumption were also recorded. We always used a large excess of NADPH over eNOSred to ensure "clean" pseudo-first-order reactions. Typical data of eNOSred reduction by NADPH are shown in Figure 1. The absorption changes were detected in several timescales and analyzed by three exponentials and a constant term at each NADPH concentration.[22] We first found a very fast component k_1 of 190 ± 40 s^{-1} at 455 nm and of the order of 400 s^{-1} at 340 nm using 100 μM NADPH (Figure 1A, insert). Given the resolution of our stopped-flow measurement (≈ 2 ms), the error on this last figure is high and we could not

(16) Porrès, L.; Alain, V.; Hapiot, P.; Blanchard-Desce, M. *Phys. Chem. Chem. Phys.* **2003**, *5*, 4576−4582.
(17) Du, M.; Yeh, H. C.; Berka, V.; Wang, L. H.; Tsai, A. L. *J. Biol. Chem.* **2003**, *278*, 6002−11.
(18) Traber, R.; Kramer, H. E.; Hemmerich, P. *Biochemistry* **1982**, *21*, 1687−93.
(19) Petrich, J.; Poyart, C.; Martin, J. L. *Biochemistry* **1988**, *27*, 4049−4060.
(20) Gutierrez, A.; Lian, L. Y.; Wolf, C. R.; Scrutton, N. S.; Roberts, G. C. K. *Biochemistry* **2001**, *40*, 1964−1975.
(21) Grunau, A.; Paine, M. J.; Ladbury, J. E.; Gutierrez, A. *Biochemistry* **2006**, *45*, 1421−34.
(22) Knight, K.; Scrutton, N. S. *Biochem. J.* **2002**, *367*, 19−30.
(23) Dunford, A. J.; Marshal, K. R. L.; Munro, A. W.; Scrutton, N. S. *Eur. J. Biochem.* **2004**, *271*, 2548−2560.
(24) Daff, S. *Biochemistry* **2004**, *43*, 3929−32.
(25) Wolthers, K. R.; Scrutton, N. S. *Biochemistry* **2004**, *43*, 490−500.
(26) Yamamoto, K.; Kimura, S.; Shiro, Y.; Iyanagi, T. *Arch. Biochem. Biophys.* **2005**, *440*, 65−78.

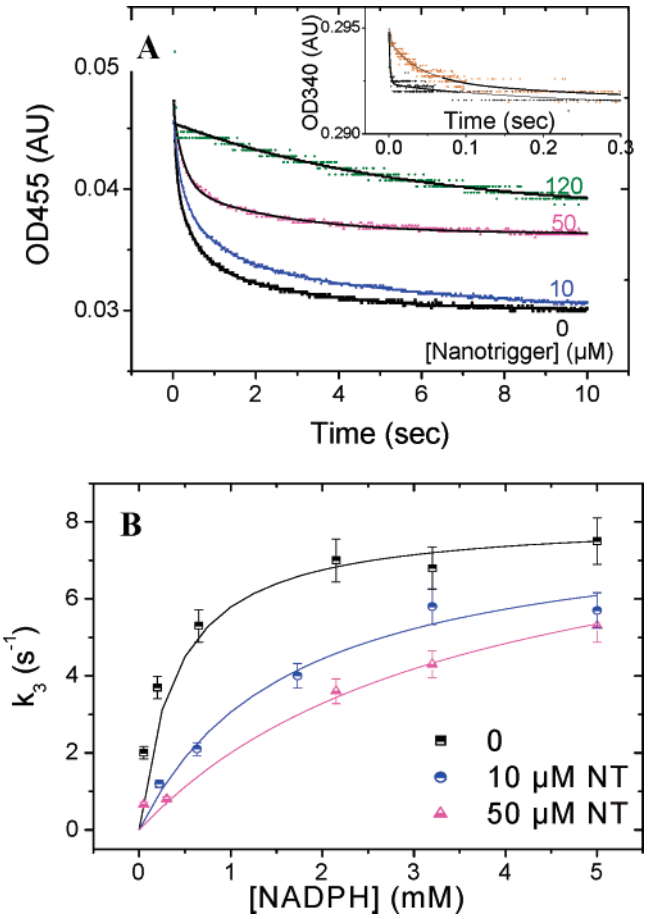

Figure 1. Competition of NT with NADPH on the NADPH site of eNOSred. (A) Raw decay of eNOSred flavin absorption monitored at 455 nm after addition of 2.15 mM NADPH to a solution of 10 μM eNOSred in the presence of 0, 10, 50, and 120 μM nanotrigger; Insert: raw decay of NADPH consumption at 340 nm after addition of 100 μM NADPH to 8 μM eNOSred alone (black) and with 8 μM NT (orange); the fits of the experimental data are shown as black lines. (B) Fit of the observed k_3 rate constant at 455 nm according to a competitive model ($k_{obs} = k_{max}$* [NADPH]/{[NADPH] + K(NADPH) * [1 + [NT]/K_i]}. The nanotrigger is taken as a competitive inhibitor, using k_{max} = 8.1, 8.1, and 9.2 s^{-1} at [NT] = 0, 10, and 50 μM, respectively, and K_i = 6.1 ± 1.5 and 7.0 ± 1.4 μM at [NT] = 10 and 50 μM.

determine this first component at higher NADPH concentrations. The second and third decay components were slower, k_2 = 14 ± 4 s^{-1} while k_3 = 1.5 ± 0.5 s^{-1} at 455 nm using 100 μM NADPH. These values determined for eNOSred are consistent with the four observed rates of 214, 27, 3.7, and 0.3 s^{-1} reported for 5 μM nNOS (without calmodulin) mixed with 50 μM NADPH.[22] Other authors reported rates of the main reduction phase in nNOS in the presence of 50 μM NADPH to be 25.8 s^{-1} at 455 nm.[27] The observed rate constants k_2, k_3 were found to follow a saturation behavior as a function of the NADPH concentration (Figure 1B and data not shown) as previously shown for other flavoproteins.[25] Peak values of 110 ± 15 s^{-1} and 8.6 ± 1.5 s^{-1} were determined for k_2 and k_3 at 455 nm, respectively.

The decay of NADPH oxidation at 340 nm and of the flavin absorption at 455 nm resulting from the addition of NADPH became slower in the presence of NT (Figure 1A). Figure 1B details the analysis obtained with k_3.[22−26] The decay rates

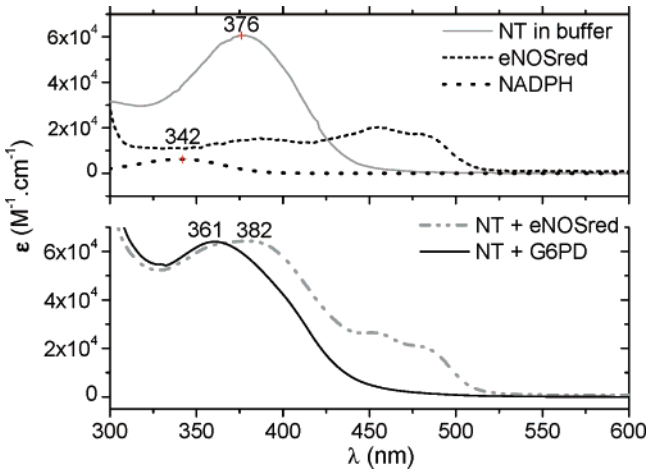

Figure 2. Selective excitation of the nanotrigger compared to the absorption of NADPH and eNOSred. (Upper panel) Dotted line, NADPH; dashed line, reductase domain of eNOS (eNOSred); full line, nanotrigger in buffer solution; note the much higher extinction coefficient of NT as compared to both NADPH and eNOSred. (Bottom panel) The (equilibrium) absorption maxima were found at λ_{max}= 382 nm and λ_{max} = 361 nm for NT bound to eNOSred and to glucose 6-phosphate dehydrogenase (G6PD), respectively, shifted from λ_{max} = 376 nm for free NT in buffer.

decreased with the increase in nanotrigger concentration. The observed k_2 rate, the step attributed to the hydride transfer reaction between NADPH (bound to the protein in step 1) and k_3 rates were best fitted by a competitive inhibition model that keeps the same limit values as those obtained in the absence of NT: k_2 = 115 ± 20 s^{-1} , k_3 = 8.6 ± 1.6 s^{-1}. The inhibition constant used to obtain the best fits (Figure 1B) is K_i = 7 ± 3 μM. Thus, the nanotrigger is an efficient competitor of eNOS catalysis initiated by NADPH.

2. Photophysics of the Bound Nanotrigger to eNOSred. a. Selective Excitation of the Nanotrigger in the Presence of eNOSred. Figure 2 compares the absorption spectra of the free nanotrigger in buffer and of NADPH. The nanotrigger possesses a ca. 10 times higher extinction coefficient of $\epsilon = 6 \times 10^4$ M^{-1} cm^{-1} at 376 nm relative to $\epsilon = 6.22 \times 10^3$ M^{-1} cm^{-1} at 340 nm of NADPH.[28] Furthermore, the absorption of the nanotrigger is well separated from that of the flavins of eNOSred,[22−24] allowing a selective excitation of the nanotrigger in the spectral range from 370 to 420 nm, and especially for the KHz laser (the 405 nm wavelength we used). The bound nanotrigger exhibits a broader absorption than that of the free NT, red-shifted to λ_{max}= 382 nm upon binding to eNOSred (Figure 2). Likewise, NT binding to eNOSred induces a red-shift of its fluorescence emission peak from 523 nm (free NT) to 533 nm (bound NT) (Figure 3A, insert). By monitoring these fluorescence changes, a binding constant of $K = (8 \pm 2) \times 10^5$ M^{-1} was obtained. This high affinity of NT for eNOSred insured that at least 80% of the nanotrigger was bound to the protein at a 1/1 stoichiometry used in the laser experiment described below.

b. Transient Absorption of Bound NT to eNOSred. Need for a Proper Control. The excited-state absorption and lifetime of the nanotrigger are expected to depend on the solvent as reported for many molecular wires.[16,29] Thus, NT has to be in an environment resembling the NADPH binding site for an accurate measurement of the rate of its natural decay k_N. The

(27) Guan, Z. W.; Kamatani, D.; Kimura, S.; Iyanagi, T. *J. Biol. Chem.* **2003**, *278*, 30859−68.
(28) Racker, E. *Methods Enzymol.* **1955**, *2*, 272.
(29) Laage, D.; Plaza, D.; Blanchard-Desce, M.; Martin, M. M. *Photochem. Photobiol. Sci.* **2002**, *1*, 526−35.

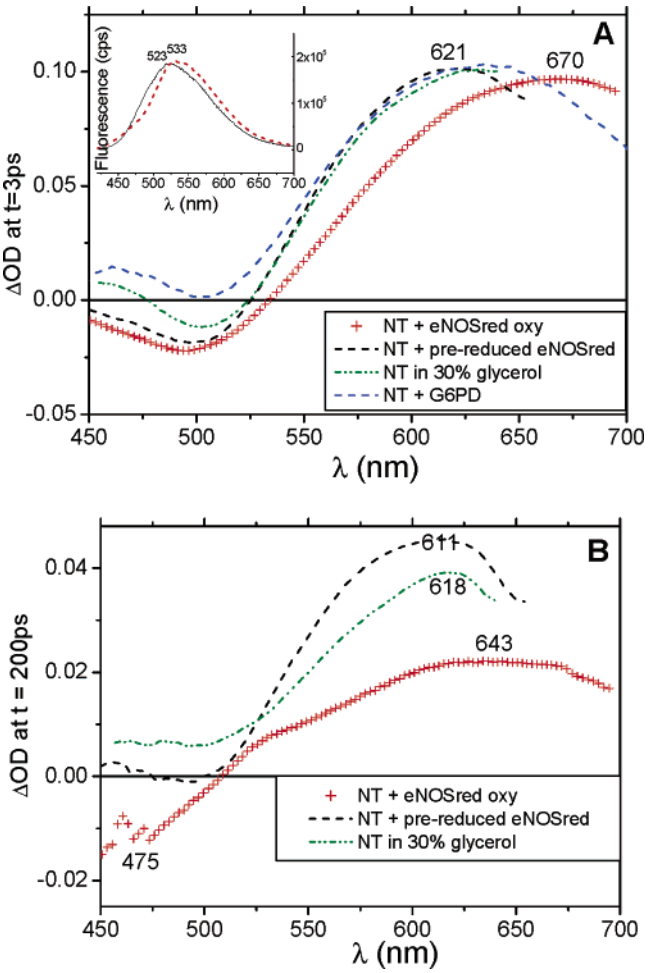

Figure 3. Transient spectra probed at 3 and 200 ps after the pump pulse for the bound NT to oxidized eNOSred compared to the controls. (A) Excited-state absorption recorded at a delay of 3 ps; note the large shift of the maxima of the (raw) spectra when NT is bound to oxidized eNOSred (λ_{max} = 670 nm, +) compared to NT in prereduced eNOSred (λ_{max} = 621 nm, black dashed) and NT in G6PD (λ_{max} = 633 nm, blue dashed); note the similar maximum at 623 nm observed when the nanotrigger is in 30% glycerol (dashed dotted). (Insert) Fluorescence spectrum of free NT (solid) and NT bound to eNOSred (dashed), consistent with the minimum observed in the transient spectrum at 490−510 nm. (B) Similar spectra as those in part A but probed 200 ps after the pump.

latter is required to extract the electron-transfer rate between NT* and FAD (F) from the observed decay rate: $k_{obs} = k_N + k_{ET}$. To confer the proper (proteic) environment to NT and NT* with minimal disturbance, we utilized the nanotrigger bound to prereduced eNOSred which already contains fully reduced flavin (F^-) that cannot be further (photo) reduced. The prereduction of the protein was achieved by light irradiation of the protein in the presence of 5 mM EDTA.[18] A maximal extent of 60% reduction could be reached by this method. This constituted our first control. The protein glucose 6-phosphate dehydrogenase (G6PD) was used as an additional control. This enzyme bears an NADP site but lacks a flavin as the electron acceptor.[30] The shift of the absorption maximum to λ_{max} = 361 nm from λ_{max} = 376 nm for free NT provided evidence of NT binding to G6PD (Figure 2). A good model for the determination of NT* excited-state properties without electron transfer is thus (see Discussion):

$$NT + h\upsilon \rightarrow NT^*$$

$$NT^* + F \xrightarrow{k_{ET}} NT^+ + F^- \qquad \text{eNOSred with oxidized FAD}$$

$$NT^* + F^- \xrightarrow{k_N} NT + F^- + h\upsilon' \qquad \text{eNOSred with prereduced FAD: Control 1}$$

$$NT^* \xrightarrow{k_N} NT + h\upsilon' \qquad \text{G6PD: Control 2}$$

Transient absorption of the bound NT to oxidized eNOSred compared to the controls.* Figure 3 compares the transient spectra monitored at 3 ps of the bound NT* to the oxidized eNOSred and NT* in the controls. Figure 3A shows that the NT* maximum was sensitive to the redox state of eNOSred, peaking at 670 nm in the oxidized eNOSred and shifted to 621 nm when eNOSred was prereduced. The excited-state absorption of NT in G6PD peaked at 633 nm while NT* in 30% glycerol, a solvent mimicking the protein interior, presented a maximum at 623 nm (Figure 3A). A minimum was observed at 490−510 nm in all samples. This minimum was attributed to the stimulated emission by comparison with the steady-state fluorescence spectrum (Figure 3A, insert).

For NT bound to oxidized eNOSred, the transient absorption decayed in two timescales, ca. 10 and 200 ps (Figure 4A, insert). In parallel with the fast 10-ps decay, a progressive blue-shift of the maximum from 670 to 643 nm was observed (see Supporting Information Figure S1). This broad 643-nm peak then decayed with no further spectral shift (Figure 3B). The transient absorption spectrum was also modified in the 450−500 nm range as shown by the comparison of the spectra recorded at 3 and 200 ps. Most of the absorption decayed at 500 nm but distinct minima at ca. 450 and 475 nm were simultaneously formed. This spectral region corresponds to the absorption of the (oxidized) flavin (FAD). The insert of Figure 4A shows the parallel decays of the transient absorption of NT* monitored at 640 nm, 600 nm, and then 478 nm where FAD absorbs. Table 1 summarizes the fit of the data with three exponentials and a constant value. The main decay was characterized by τ_3 = 110 ± 26 ps, reaching subsequently an asymptotic value (Figure 4A). This main component accounted for ∼50−60% of the signal at 600 nm, whereas shorter time scale components τ_1 = 1.3 ± 0.5 ps and τ_2 = 7 ± 3 ps represented 30% and ∼10% of the total absorption changes, respectively (insert).

The transient spectrum of NT in prereduced eNOSred decayed more slowly than in oxidized eNOSred (compare Figure 4A and B). The absorption maximum decayed away in hundreds of picoseconds, characterized by τ_3 = 400 ± 100 ps obtained for eNOSred at 60% prereduction. Moreover, in the case of prereduced eNOSred, the slow decay monitored at 620 and 600 nm differed drastically from the fast decay followed at 478 nm (Figure 4B and Table 1), without correlated decays observed for NT* and FAD in oxidized eNOSred.

We also used NT bound to G6PD to monitor the rate of decay of NT* in the absence of electron transfer. The insert of Figure 4B compares the decays of NT* in prereduced eNOSred with that in G6PD at 600 and 478 nm. Both controls presented a similar slow decay in the hundreds of picoseconds, characterized

(30) Kotaka, M.; Gover, S.; Vandeputte-Rutten, L.; Au, S, W. N.; Lam, V. M. S.; Adams, M. J. *Acta Crystallogr., Sect. D* **2005**, *61*, 495−504.

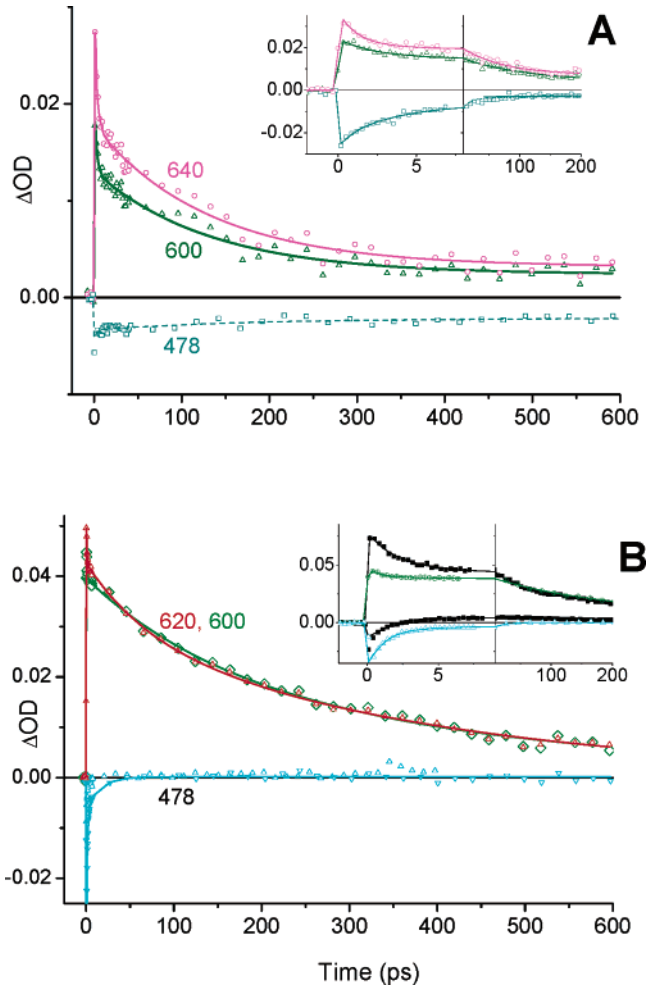

Figure 4. Faster decay of the transient absorption of the bound nanotrigger to oxidized eNOSred (A) compared to the controls (B). (A) (Raw) decays observed at 640 nm (magenta), 600 nm (green), and 478 nm (cyan) with NT in oxidized eNOSred; the main panel shows data recorded at the time scales of 50 and 600 ps, and the insert presents the same experiments with 10 and 200 ps timescales. (B) Decays monitored at 620 nm (red), 600 nm (green), and 478 nm (cyan) of NT in the presence of prereduced eNOSred at the extent of 39% reduction; the insert presents the same experiments at 10 and 200 ps timescales (with the same colors); superimposed in the insert, the decay of NT* bound to G6PD (shown in black) is monitored at 600 nm (positive signal) or at 478 nm (second control); the full lines represent the fit of the data summarized in Table 1. [eNOSred] = 12 μM = [NT], 50 mM Tris buffer at pH = 7.5 containing 150 mM NaCl, 5% glycerol; [G6PD] = 117 μM, [NT] = 25 μM in buffer containing 1 mM glucose 6-phosphate and 0.3 mM $MgCl_2$.

by $\tau_3 = 400 \pm 60$ ps but differed by the value of the second lifetime $\tau_2 = 54 \pm 15$ ps, longer in G6PD than in prereduced eNOSred $\tau_2 = 20 \pm 7$ ps (Table 1).

The shorter lifetime $\tau_3 = 110 \pm 26$ ps for NT* in oxidized eNOSred than in the two controls ($\tau_3 = 400 \pm 60$ ps) supported the attribution of the third kinetic phase to electron transfer. The minor component of NT*, $\tau_2 = 7 \pm 3$ ps, shortening in oxidized eNOSred as compared to prereduced eNOSred or NT* in G6PD remained puzzling. The large spectral shift only observed during that time scale for NT* in oxidized eNOSred suggested a possible excited-state complex. One critical residue inserted between the NADPH and FAD in eNOSred is Phe1160. To confirm the above attribution of electron transfer to the main (third) step and to support the hypothesis of an excited-state complex between NT* and Phe1160, we used the oxidized

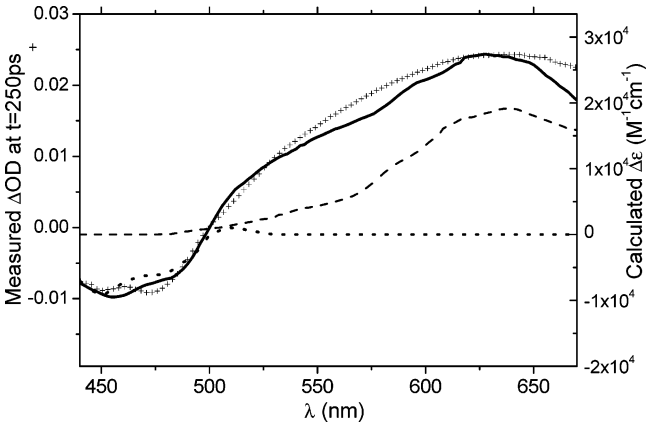

Figure 5. Comparison of the experimental and calculated transient spectra: left scale indicates absorbance changes of spectral raw data monitored 250 ps after the pulse, crosses; right scale represents the sum of (60% NT cation + 40% dication + (reduced − oxidized flavin) − (reduced NT), solid line; the experimental data were corrected for the direct excitation of the protein. The spectrum of the cation of the NT chromophore was generated by chemical oxidation with $SbCl_5$ in CH_2Cl_2 (dashed line, the dication is omitted for clarity); the dotted line represents the absorption difference of the (unprotonated) semireduced − oxidized flavin.

reductase domain of eNOS in which Phe1160 was replaced by Ala or F1160A mutant eNOSred. NT* bound to F1160A yielded $\tau_2 = 20 \pm 4$ ps and $\tau_3 = 190 \pm 20$ ps (Table 1). NT bound to F1160A showed a similar τ_2 relative to that found in NT bound to prereduced eNOSred, consistent with lacking complex formation in the mutated F1160A as in prereduced eNOSred. Consequently, no significant spectral shifts were observed (data not shown). These data supported the hypothesis of an excited-state complex between NT* and Phe1160 attributable to a minor component, τ_2. Moreover, a swinging of Phe1160 away from both NADPH and FAD is likely to make room for the bound nanotrigger, accounting for the main component of NT*.

The attribution of the main decay step (third step) to ET implies that the transient spectra monitored 250 to 600 ps after NT excitation correspond to the sum of the oxidized and reduced species of the donor and acceptor pair corrected for the bleaching of the reduced NT and oxidized eNOSred. NT is able to give electron(s) but unable to transfer a proton to the flavin. It is thus assumed that FAD is reduced but not protonated in the experiment.[31] The spectra of the cation and dication species of NT were determined by chemical methods. The nanotrigger was designed to reduce proteins with one or two electrons, and two oxidation states have been reported for the related chromophore MC.[16] The redox activity of NT is localized in the chromophore moiety, justifying our attempts to oxidize it and the further assumption that the oxidized species of NT chromophore are identical to that of the whole NT molecule. The NT chromophore was chemically oxidized with $SbCl_5$ yielding the dication and monocation, the latter absorbing at $\lambda_{max} = 640$ nm. Figure 5 shows the fit of the experimental spectrum monitored at 250 ps (crosses) with the calculated sum of the absorption of the oxidized nanotrigger species plus the reduced flavin. This sum estimated correctly the experimental maxima and minima of the transient difference spectrum; discrepancies around 575 nm introduced uncertainties in the extent of the dication, ranging from 25% to 40% of the oxidized NT, varying the corresponding amount of the monocation from 75 to 60% accordingly.

(31) Sakai, M.; Takahashi, H. *J. Mol. Struct.* **1996**, *379*, 9−18.

Table 1. Kinetic Parameters for the Decay of NT* Bound to eNOSred and to Controls at Various Wavelengths[a]

NT in protein	% prereduction	λ (nm)	ΔOD_{max}	A_1	τ_1 (ps)	A_2	τ_2 (ps)	A_3	τ_3 (ps)	cte
prereduced eNOSred	39	600	0.0255	0.20	1.1	0.35	142	0.45	551	0
		620	0.0281	0.40	1.7	0.39	97	0.21	673	0
		510	−0.0255	0.69	1.7	0.15	13	0.15	471	0
	60	600	0.0271	0.23	0.8			0.77	347	0
		620	0.032	0.39	0.8			0.61	320	0
		510	−0.0196	0.58	1.8	0.14	27	0.28	400	0
		478	−0.0065	0.76	2.0			0.24	447	0
G6PD[b]	-	600	0.020	0.40	2.0	0.25	54	0.35	410	0
		478	−0.0072	0.80	1.8			0.20	400	0
eNOSred (oxidized)	0	600	0.0254	0.28	0.6	0.10	6.2	0.44	106	0.18
		620	0.0294	0.33	1.3	0.07	8.0	0.50	118	0.10
		640	0.0320	0.40	1.8	0.03	7.0	0.46	101	0.10
		510	−0.0041	0.85	2.0			0.14	110	0.01
		478	−0.0045	0.80	1.1			0.06	107	0.13
F1160A (oxidized)	0	600	0.0163	0.26	2.1	0.14	27	0.56	168	0.03
		620	0.0264	0.41	2.1	0.16	20	0.42	200	0.01

[a] The sum of the amplitude terms $A_1 + A_2 + A_3$ + cte was normalized to 1. [eNOSred] = (10−20) μM, [eNOSred]/ [NT] = 1. [b] [G6PD] = 117 μM, [NT] = 25 μM in buffer containing 1 mM Glucose 6-phosphate and 0.3 mM $MgCl_2$.

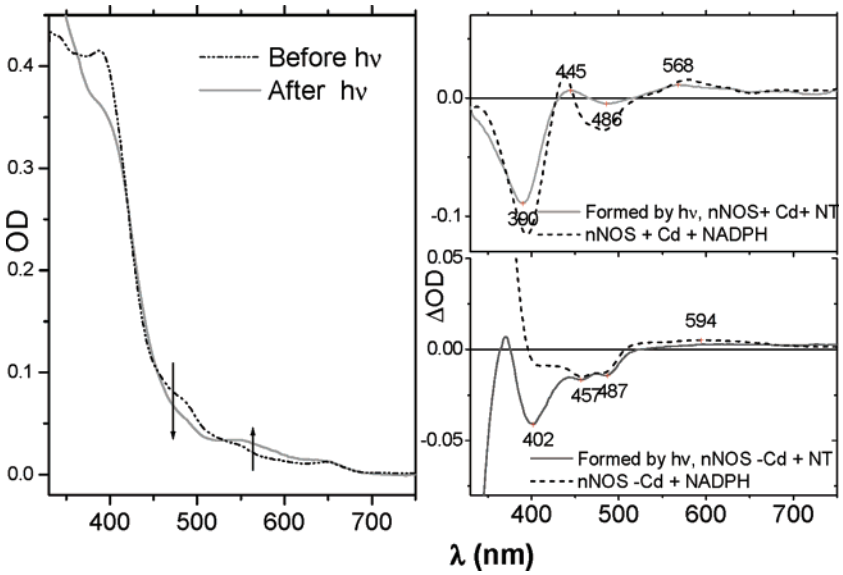

Figure 6. Light-induced reduction of the flavin and heme of WT eNOS by NT. An aerated solution of 3.4 μM nNOS containing 1 mM NOHA, 50 μM BH_4, Ca^{2+}/calmodulin (Cd), and 5μM NT was irradiated at 400 nm with a 50 W halogen lamp equipped with a BG12 interference filter. The left panel shows the absorption spectra recorded before (dashed dotted) and after (solid) irradiation. Note the decrease in the flavin bands and the increase of the broad visible α band, consistent with reduction of the heme. The difference spectrum formed by irradiation, shown in the upper right panel (solid), presents similar maxima in the Soret and α bands as that obtained by addition of NADPH to nNOS (2.5 μM) in the presence of NOHA, BH_4, and Cd shown as a reference (dashed). The bottom right panel shows the difference spectrum obtained after irradiation of nNOS in the absence of Ca^{2+}/calmodulin in the presence of NT (solid) or obtained with NADPH in the absence of NT and light (dashed). Note that in this case only the flavins were reduced by NT, the absence of calmodulin blocking the (photoinduced) electron flow from the reductase to the oxygenase domain.

c. Light Irradiation of nNOS in the Presence of NT. The above ultrafast kinetics demonstrated the electron transfer from NT to FAD after excitation with a laser pulse. To ensure that this excitation triggered the electron flow associated with NOS catalysis, steady-state irradiation experiments were performed in an aerated solution of full length nNOS in the presence of *N*-hydroxyarginine, NOHA, and BH_4. We used nNOS instead of eNOS because the ferrous nitrosyl complex was shown to be formed in the steady-state catalysis of nNOS.[30] The difference spectra monitored before and after addition of NADPH (in the absence of NT and light) were compared to those obtained before and after light irradiation in the presence of NT (without NADPH). In the absence of calmodulin, thus the electron flow from the reductase domain cannot activate the oxygenase domain; consequently, only the flavins got reduced either by NADPH or by light activation with NT, as shown by the bleaching of the oxidized flavins at 457 and 487 nm (Figure 6, bottom right panel). In the presence of calmodulin, the NADPH-induced catalysis yielded the ferrous nitrosyl complex with the typical absorption difference in the Soret band at 440 nm and the broad visible band at ca. 575 nm. These maxima are similar to those monitored after irradiation in the presence of NT, peaking at 445 and 568 nm with minima at 390 and 486 nm. The formation of a single broad visible band at 568 nm is typical for a reduced heme (partly) nitrosylated, and the 486 nm minimum accounts for the reduction of flavins (left panel). Both the disappearance of the reduced NT and the oxidized heme Soret band likely contributed to the minimum at 390 nm (upper

Scheme 3. Decay Mechanism of the Protein-Bound NT*

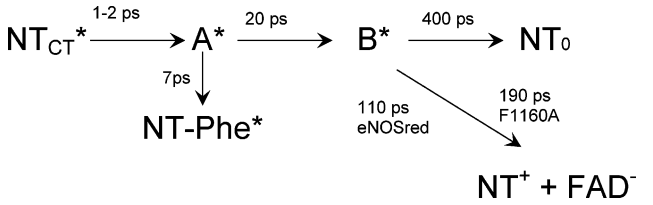

[a] In the presence of eNOSred, A* decays in 7 ps to a complex NT-Phe* or to B* in prereduced eNOSred and in glycerol. NT-Phe* deactivates to the ground state via presently unidentified (radiative and nonradiative) processes. B* returns to the ground state NT_0 in prereduced eNOSred or undergoes ET in oxidized eNOSred. Similar steps, except the conversion of A* to B* were also found in F1160A.

right panel). Thus, irradiation of NT bound to nNOS induced heme reduction and subsequent formation of some heme−NO complex, as attested by absorption spectroscopy.

Discussion

Innovative Design of the Nanotrigger: The nanotrigger was designed according to a number of criteria listed below and substantiated by the experimental data:

(1) Selective Excitation. A selective excitation of the nanotrigger is possible, due to a high extinction coefficient combined with a maximal absorption shifted from that of eNOSred (Figure 2).

(2) Specific Binding to the NADPH Site of the Protein. The stopped-flow experiments support the specific binding of the nanotrigger to the NADPH site: a direct competition between the nanotrigger and NADPH on its natural binding site was observed with an inhibition constant of $K_i = 7 \pm 3\ \mu M$ (Figure 1). Our competition kinetic results are consistent with a higher affinity of NT for the NADPH site than the natural cofactor as judged by the comparison of K_i with K_M[23] as well as the binding constant of $K = (8 \pm 2) \times 10^5\ M^{-1}$ determined for NT by fluorescence.

(3) Light-Induced Electron Transfer from the Nanotrigger to the Protein Initiated the Enzymatic Activity. To calculate the electron-transfer rate between NT* and FAD (F) from the observed decay rate, the rate of natural decay k_N of the nanotrigger was determined in an environment resembling the NADPH binding site. NT in prereduced eNOSred was used as our first control. Experimental difficulties limited the extent of flavin prereduction to more than 60%. This incomplete prereduction could actually lead to an underestimation of k_N. Therefore, NT in G6PD was taken as a second control. This protein carries an NADP site[30] but lacks FAD as an electron acceptor. This enzyme converts glucose 6P to 6-phosphoglucono-lactone while reducing $NADP^+$ to NADPH and definitely is not a reductase. Moreover, inspection of its structure did not reveal a nearby alternative aromatic residue that could function as an electron trap. Evidence for NT binding to G6PD was given by the blue shift of the absorption to 361 nm as compared to 376 nm for NT in buffer (Figure 2). Thus, G6PD-bound NT served as an additional control for the determination of k_N.

Evidence for the photoinduced electron transfer is supported by three consistent data sets.

First, the main decay of the transient absorption is faster when the nanotrigger is bound to oxidized eNOSred as compared to that observed in the controls (Figures 3, 4 and Scheme 3).

NT* transient absorption decays to zero in three steps in the absence of electron transfer. The first excited state NT_{CT}* has the shortest lifetime, $\tau_1 = 1.0-2.0$ ps. Similar lifetimes of 2 to 3 ps have been reported for polyenes substituted with donor and acceptor end groups and attributed to a charge transfer state.[29] In contrast, the *p*-coumaric acid chromophore of the photoactive yellow protein readily isomerizes by twisting in 1 ps.[32] In NT, τ_1 is unaffected within experimental error by an increase of the viscosity up to 60% glycerol, showing that this first excited state is likely to be a (trans) charge transfer state.

The second lifetime A* is shortened to $\tau_2 = 7 \pm 2$ ps in oxidized eNOSred compared to $\tau_2 = 20 \pm 4$ ps in prereduced eNOSred and in F1160A (Table 1). Thus, this second step is attributed to an excited-state complex (NT-Phe)* that contributed to only a minor part 11% of the eNOSred decay and was absent in F1160A. It probably reflected a minor Phe conformation stacked on FAD, unproductive for ET and therefore not found in prereduced eNOSred. The extended shape of NT required for an effective charge delocalization probably locked the NADPH site in an active conformation with most of the Phe1160 moved away from NT.

The third component is the most significantly shortened in comparison with the control and represented the main decay (45−60%) at 600 nm (Table 1). The ET rate was estimated from the difference: $(1/110 \times 10^{-12}) - (1/400 \times 10^{-12}) = (7 \pm 2) \times 10^9\ s^{-1}$ in eNOSred, based on $\tau_3 = 400 \pm 100$ ps for NT in prereduced eNOSred and confirmed by the use of G6PD (Table 1). Phe residues are usually found redox inert in contrast to Trp or Tyr,[33] consistent with electron transfer taking place in F1160A but at a slower rate $\tau_3 = 190 \pm 20$ ps. This result showed that F1160 was not involved in the electron transfer and identified FAD itself as the electron acceptor. The fit of the experimental transient spectrum involving the reduced FAD confirmed this assertion (Figure 5 and see below).

The ET yield was estimated from the remaining absorption at 600 ps using $\Delta\epsilon(600) = 2.6 \times 10^4\ M^{-1}\ cm^{-1}$ relative to that of MbCO as a reference (assuming a quantum yield (Φ) of CO photodissociation of 1), $\Phi = 0.19 \pm 0.05$ and $\Phi = 0.09 \pm 0.03$ in WT oxidized eNOSred and F1160A, respectively. This difference in yield suggested that some charge recombination likely took place within 600 ps in F1160A; this is consistent with a structural role of Phe1160 in optimizing the conformation of the NADPH site for ET.

The second evidential support for electron transfer is the proper fit of the experimental transient spectrum with the sum of (semireduced − oxidized)flavin + (monocation + dication radical of NT) (Figure 5); in this calculation, we assume that the protonation of FAD does not occur in the time scale of our experiment.[29] The calculation showed that 25 to 40% of NT yielded the dication, with concomitant delivery of two electrons. The mechanism of this process will require further investigations since the presence of the dication may result from alternative pathways, either by two sequential (photoinduced) electron transfers or by an intrinsic instability of the cation when dissociated from the protein milieu to the solution.[16] Thus, the

(32) Lee, I. R.; Lee, W.; Zewail, A. H *Proc Natl. Acad. Sci. U.S.A.* **2006**, *103*, 258−62.
(33) Byrdin, M.; Eker, A. P. M.; Vos, M. H.; Brettel, K. *Proc. Natl. Acad. Sci. U.S.A.* **2003**, *100*, 8676−81.

presence of the dication in addition to the monocation may arise by its diffusion out from eNOSred and thus reflect the k_{off} rate of the NT.

Third, evidence of electron transfer is given by the shift of NT* maximum to 670 nm when ET occurs as observed in oxidized eNOSred or in F1160A in contrast to 620 nm as a maximum observed in the controls lacking electron transfer (Figures 3 and 5). Thus, the excited state in the controls presented only a partial charge delocalization over the chromophore chain. In contrast, the large shift of the NT* maximum attested to a complete charge delocalization in the excited state required for charge separation (ET) in oxidized eNOSred.

Concluding Remarks

In this work, the successful targeting of the designed nanotrigger to the NADPH site of eNOSred and its subsequent photoactivation by light are demonstrated. Such a compound enables a time-resolved study of electron transfer within the reductase domain of NOS, which contains a number of negative regulating elements. Protein activation is selectively and rapidly triggered at the natural site by light absorption of the nanotrigger; this should allow detection of short-lived intermediate(s) that would not be possible with NADPH or with diffusion-limited compounds like caged nucleotides because of their (relatively) slow activation and the slow rate-limiting binding step. Furthermore, the rapid electron transfer mainly bypasses the slow hydride transfer and thus is very useful to investigate the subsequent electron-transfer events of NOSred or the full length NOS. The photoinduced electron transfer is faster than that reported for the rhenium-diimine wires, although the redox partner is not the same in both cases: FAD in the present study, compared to the heme in the latter case.[5] The selective binding to the NADPH site by NT should enable activation of other proteins involved in bioreductive reactions as suggested by the binding of NT to G6PD. Such a versatile tool is also expected to be useful for time-resolved X-ray crystallography, presently limited to the study of proteins with slow turnover.[3] Work along these lines is in progress in our laboratories.

Acknowledgment. The authors gratefully acknowledge Dr. Marc Lebret for preliminary modeling studies, Dr. Yves Meshulam for his help with the stopped-flow experiments, and Dr. Viatcheslav Jouikov for electrochemical measurements.

Supporting Information Available: Experimental details: Transient absorption spectra. This material is available free of charge via the Internet at: http://pubs.acs.org.

JA067543E